Retina

Restoration of Cone Interdigitation Zone Associated With Improvement of Focal Macular ERG After Fovea-Off Rhegmatogenous Retinal Reattachment

Azusa Kominami, Shinji Ueno, Taro Kominami, Ayami Nakanishi, Chang-Hua Piao, Eimei Ra, Shunsuke Yasuda, Tetsu Asami, and Hiroko Terasaki

Department of Ophthalmology, Nagoya University Graduate School of Medicine, Nagoya, Japan

Correspondence: Shinji Ueno, 65 Tsuruma-Cho, Showa-ku, Nagoya 466-8550, Japan;
ueno@med.nagoya-u.ac.jp.

Submitted: December 26, 2015
Accepted: February 26, 2016

Citation: Kominami A, Ueno S, Kominami T, et al. Restoration of cone interdigitation zone associated with improvement of focal macular ERG after fovea-off rhegmatogenous retinal reattachment. *Invest Ophthalmol Vis Sci*. 2016;57:1604–1611. DOI: 10.1167/iovs.15-19030

Purpose. To determine whether a correlation exists between the parameters of the focal macular ERGs (FMERGs) and the microstructural changes of the photoreceptors after successful surgery for fovea-off rhegmatogenous retinal detachment (RRD).

Methods. Twenty eyes of 20 patients who had undergone successful surgery to reattach the retina in eyes with fovea-off RRD were studied. Focal macular ERGs and spectral-domain OCT (SD-OCT) were recorded at 1 and 6 months after the surgery. Changes of the components of the FMERGs, as well as changes of the SD-OCT parameters including the length of the external limiting membrane (ELM), ellipsoid zone (EZ), cone interdigitation zone (CIZ), and size of the outer photoreceptor area (between ELM and RPE), were determined.

Results. During the postoperative period, the mean amplitudes of the a-waves increased by 1.4 times and the b-waves by 1.7 times. Spectral-domain OCT showed that the mean length of the EZ and CIZ and the size of the outer photoreceptor area had increased significantly at 6 months. The degree of the increase in the CIZ and outer photoreceptor area was significantly correlated with the increase in the amplitudes of the b-waves of the FMERGs ($r = 0.56$, $P = 0.042$, $r = 0.57$, $P = 0.040$, respectively; Spearman rank correlation test). However, the length of the EZ was not significantly correlated with the increase of the b-waves.

Conclusions. A restoration of the EZ alone might not be enough to improve the FMERGs, and a restoration of the EZ accompanied by that of the CIZ was essential for the recovery of the FMERGs after fovea-off RRD.

Keywords rhegmatogenous retinal detachment, focal macular electroretinogram, spectral domain optical coherent tomography, cone interdigitation zone

Rhegmatogenous retinal detachment (RRD) is a vision-threatening morphologic abnormality that requires surgery for reattachment. The success rate of retinal reattachment by either scleral buckling or pars plana vitrectomy (PPV) is approximately 90%.[1,2] However, even after successful reattachment, the visual function may not fully recover. Occasionally, poor visual acuity and/or metamorphopsia persists postoperatively, especially in cases of RRD with the fovea off.[3–7]

Experimental studies in both animals and humans have shown that retinal detachment causes a loss of the outer segments of photoreceptor cells,[8–12] but the exact cause for the reduction of visual function has not been determined.

Recent advances in optical coherence tomography (OCT), especially spectral-domain OCT (SD-OCT), have enabled clinicians to evaluate the alterations of the microstructures of the retina directly. Recent OCT studies have shown that disruptions of the external limiting membrane (ELM), ellipsoid zone (EZ), and cone interdigitation zone (CIZ) of the photoreceptors were correlated with decrease in visual acuity after surgery.[3,5,13–19] The results of other studies have shown that restoration of the EZ of the photoreceptor and a thickening of the fovea are associated with the recovery of best-corrected visual acuity (BCVA) after reattachment of a RRD.[5,20,21] These results suggested that the recovery of retinal function after retinal reattachment depended on the degree of regeneration of the outer photoreceptor layer.

However, an important limitation of these previous studies was that the visual functions were evaluated subjectively. Measurements of the visual acuity and perimetry are relatively simple procedures and are commonly used to assess visual function, but they are subjective tests. In addition, these tests might be affected by other conditions such as cataracts, vitreous haze, and astigmatism. Microperimetry can be used to evaluate the retinal function of a very small area, but it is also a subjective method.[3,14,22]

The electroretinogram (ERG) is commonly used to assess the physiological status of the retina objectively, and many studies have evaluated the retinal physiology after retinal detachment and reattachment surgery using full-field ERGs[23] and multifocal ERGs.[24–27] However, these studies did not examine the relationship between the retinal physiology and the OCT-determined morphologic alterations of the outer retina.

Focal macular ERGs (FMERGs) are composed of a- and b-waves, oscillatory potentials (OPs), and other components, and they can be used to evaluate the physiological status of the macula objectively.[28] Focal macular ERGs have been used to analyze the physiology of the macula in many diseases.[29–34] Focal macular ERGs assess the physiology of the entire macular

Investigative Ophthalmology & Visual Science

area, and their properties may not correspond to the BCVA, which depends on the functioning of only the central fovea.

This study aimed to determine the correlation between the macular physiology determined by FMERGs and the integrity of the microstructures of the photoreceptor layer analyzed by SD-OCT. To accomplish this, we studied 20 patients with fovea-off RRD and recorded the FMERGs and the SD-OCT images after successful reattachment of the detached retina. We shall show that the recovery of the FMERGs was significantly associated with the recovery of the CIZ of the photoreceptors.

Patients and Methods

We reviewed the medical records of 20 eyes of 20 consecutive patients who underwent surgery for fovea-off RRD and were followed with FMERG and SD-OCT recordings. The patients were examined between March 2013 and September 2014 at the Nagoya University Hospital. All of the patients signed an informed consent for the surgery and agreed to have their visual acuity, FMERGs, and SD-OCT recorded during the follow-up period of 6 months. The procedures used in this study were approved by the Institutional Review Board of Nagoya University Graduate School of Medicine (approval No. 2015-0294). All of the procedures conformed to the tenets of the Declaration of Helsinki. A written informed consent was obtained from all the patients after they were provided with information on the procedures to be used.

All the patients had standard ocular examinations including measurements of the BCVA, visual field tests with Goldmann perimetry, fundus photography, fundus examinations with indirect ophthalmoscopy, slit-lamp biomicroscopy, SD-OCT, and B-scan ultrasonography at the time of diagnosis. Spectral-domain OCT was used to confirm that the fovea was off in the eyes with RRD.

The postoperative examinations were performed at 1 week, 1 month, 2 months, 3 months, and 6 months at least. The BCVA and the fundus were examined at each follow-up examination. Spectral-domain OCT and FMERGs were recorded at 1 and 6 months after the surgery. A standard Japanese visual acuity chart was used, and the decimal BCVA was converted to the logarithm of the minimum angle of resolution (logMAR) for the statistical analyses.

Surgical Procedures for Retinal Reattachment Surgery

Standard 3-port PPV was performed with a 25-gauge system (Constellation; Alcon Labs, Fort Worth, TX, USA) on 13 eyes. Cataract surgery by phacoemulsification and intraocular lens implantation was performed prior to the PPV when the cataract was visually significant. After the PPV, 20% SF6 gas was used to tamponade the retina, and the patients were instructed to remain in a prone position for at least 3 days.

Scleral buckling with cryopexy was performed on seven eyes. During the scleral buckling surgery, any subretinal fluid was drained and 0.6 mL 100% sulfur hexa-flouride (SF6) gas was used to tamponade the retina in one case with bullous retinal detachment. All of the patients had a complete retinal reattachment after the initial operation. All of the surgeries were performed on the day of or 1 day after the diagnosis.

Focal Macular Electroretinograms

Focal macular ERGs were recorded from both eyes at 1 month and only the affected eye at 6 months after the surgery. The procedures for recording the FMERGs (ER-80; Kowa, Nagoya, Japan) have been described in detail.[31–34] Briefly, the pupils were fully dilated with 0.5% tropicamide and 0.5% phenylephrine hydrochloride. A Burian-Allen bipolar contact lens electrode (Hansen Ophthalmic Development Laboratories, Iowa City, IA, USA) was used to record the FMERGs. The size of the stimulus spot was 15°, the luminance of the stimulus was 30 cd/m^2, the background was 3 cd/m^2, and the stimulus duration was 100 ms. Electroretinograms were recorded with the room lights on, and thus the responses were recorded under photopic conditions.[33] The position of the stimulus spot on the fundus was monitored during the recording with a modified infrared fundus camera.

The responses were recorded with digital bandpass filters set at 5 to 500 Hz for the a- and b-waves, and 500 responses were averaged at a stimulation rate of 5 Hz (Neuropack S1 MEB-9400; Nihon Kohden, Tokyo, Japan). The components with frequencies < 70 Hz were extracted from the FMERGs by Fast Fourier Transform (FFT). This process allowed us to isolate and measure the amplitudes and implicit times of the a- and b-waves by excluding OPs and high-frequency noises.

The a-wave amplitude was measured from the baseline to the first negative trough, and that of the b-wave was measured from the trough of the a-wave to the next large positive peak. The implicit times of the a- and b-waves were measured to the trough of the a-wave and peak of the b-wave.

SD-OCT Measurements

Cross-sectional images of the retina obtained by Spectralis (Heidelberg Engineering, Heidelberg, Germany) or RS-3000 Advance (NIDEK, Gamagori, Japan) were evaluated. The same type of instrument was used to follow a given patient. One hundred SD-OCT scans were averaged for each OCT image using the eye tracking system. Horizontal and vertical scans through the center of the fovea were obtained within an extent of 30° angle by the Spectralis and 6-mm length by the RS-3000 Advance. We analyzed the SD-OCT images within 2250 μm from the fovea or 4500 μm in total length. We analyzed this area because the focal ERGs were elicited by a circle whose diameter was approximately 4500 μm, which was calculated for eyes with the distance from the lens to the retina of 17 mm.

We measured the length of the intact ELM, EZ, and CIZ. We also measured the outer photoreceptor area. The lengths of the ELM, EZ, and CIZ were measured by the intensity profile of each line that was extracted from the SD-OCT images. To do this, we selected the visible ELM, EZ, CIZ, and RPE manually with the ImageJ software[35] (version 1.48; http://imagej.nih.gov/ij/; provided in the public domain by the National Institutes of Health, Bethesda, MD, USA), and selected the intensity data of these lines separately with the "Plot profile" tool of ImageJ. Then we obtained the "column average plot," in which the *x*-axis represented the horizontal distance through the line and the *y*-axis represented pixel intensity. The pixel intensity data were moved from the ImageJ file to an Excel file (Excel 2013; Microsoft, Inc., Redmond, WA, USA), and the intensity of each pixel was determined by averaging the intensities of four adjacent pixels. Representative SD-OCT images and intensity profiles obtained by this method at 1 month are shown in Figures 1A, 1C, and 1E, and at 6 months in Figures 1B, 1D, and 1F. We compared the intensity of each pixel with the intensity of the RPE in the corresponding area using Excel. If the intensity of the ELM was more than 0.2 times that of the RPE intensity, we concluded that the ELM was present. In the same way, we set 0.6 times the RPE intensity for the EZ and 0.8 times the RPE intensity for the CIZ. If the line was not visible, we concluded that the line was absent. We selected these intensity values by the intensity profiles of the fellow eyes; we set the lower limit to a level where all of the visible EZ, CIZ, and ELM were

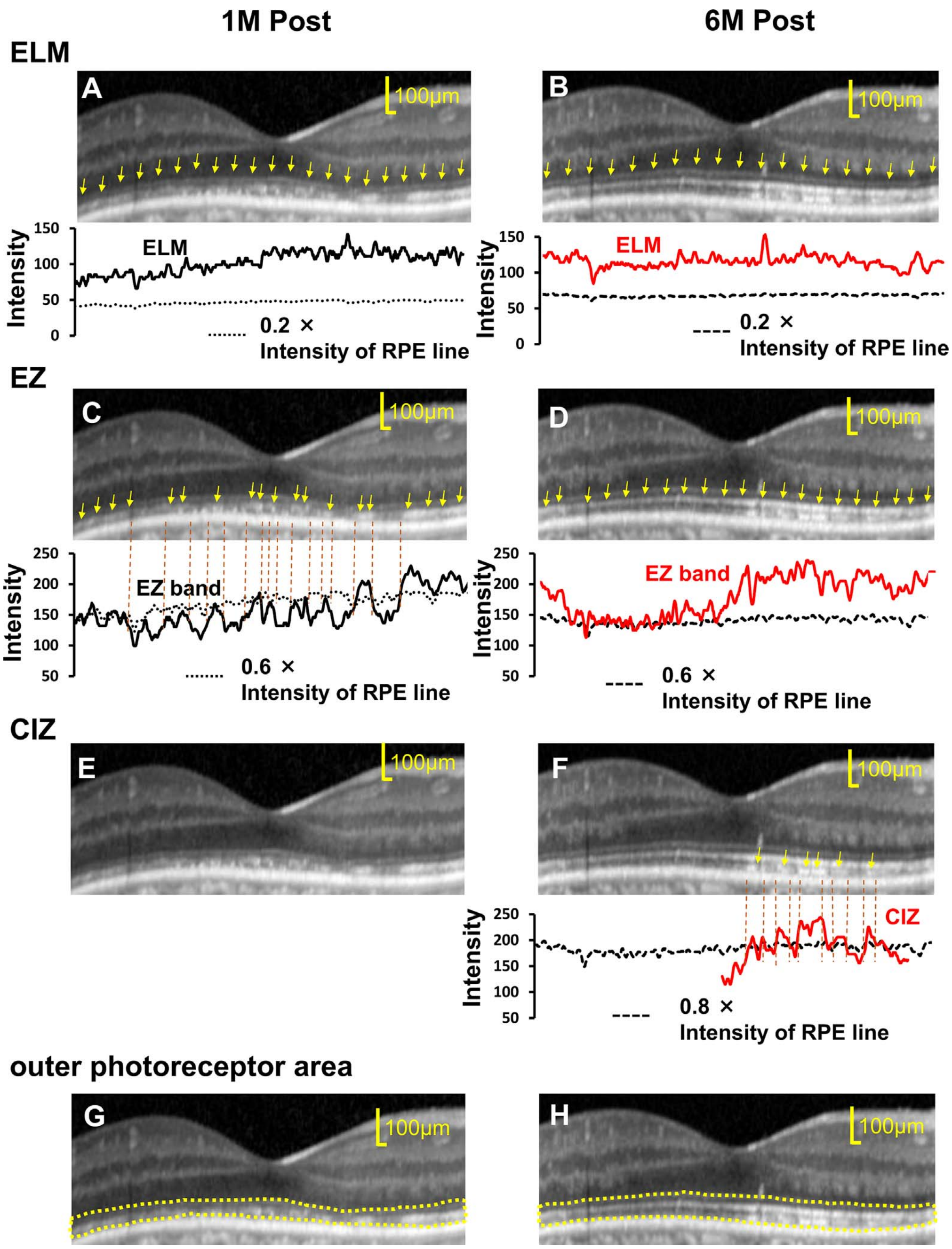

FIGURE 1. Changes in spectral-domain optic coherence tomographic (SD-OCT) images of representative eyes with a fovea-off rhegmatogenous retinal detachment. (**A**, **C**, **E**, **G**) SD-OCT images at 1 month postoperative, which are essentially the same. (**B**, **D**, **F**, **H**) Images at 6 months postoperative. The measurement procedures for ELM, EZ, CIZ, and the outer photoreceptor area are shown. (**A**, **B**) *Arrows* in the SD-OCT images point to the ELM, and the corresponding intensity profiles in grayscale are shown *below.* If the intensity of ELM exceeded 0.2 times the intensity of RPE line (*dashed line*) in the corresponding pixel, we judged that the ELM was present. (**C**, **D**) *Arrows* in the SD-OCT images point to the ellipsoid zone (EZ), and the corresponding grayscale intensity profiles are shown *below.* If the intensity of the ELM exceeded 0.6 times that of the RPE line (*dashed line*) in the corresponding pixel, we judged that the EZ was present. (**E**, **F**) *Arrows* in the SD-OCT image of (**F**) point to the cone interdigitation zone (CIZ), and the corresponding grayscale intensity profiles are shown *below.* If the intensity of the CIZ exceeded 0.8 times that of the RPE line (*dashed line*) in the corresponding pixel, we judged that the CIZ was present. Where the line was not visible, we judged that the line was absent. (**G**, **H**) Outer photoreceptor areas at 1 month and 6 months are shown within the surrounding *dashed line*.

included. We calculated the sum of the length of the ELM, EZ, and CIZ from the Excel data.

How we measured the outer photoreceptor area in the areas surrounded by the dashed line is shown in Figures 1G and 1H. The outer photoreceptor area was defined as the area between upper surface of the RPE and the ELM, and the area was measured by ImageJ software.[35] The length and area were measured in pixels and converted to metric units (μm) using the resolution (μm/pixel) fixed in the software of each OCT instrument. The measurements of each component were performed from the horizontal and vertical scan images, and the average value from two images was used in the statistical analyses.

Table. Clinical Data of Patients With Fovea-Off Rhegmatogenous Retinal Detachment

Number of patients/eyes, *n* (%)	*n* = 20
Right eyes	13 (65)
Left eyes	7 (35)
Sex, *n* (%)	
Male	16 (80)
Female	4 (20)
Age, y, mean ± SD [range]	54.50 ± 13.67 [26 to 75]
Extent of retinal detachment, *n* (%)	
1 quadrant	1 (5)
2 quadrants	12 (60)
3 quadrants	7 (35)
4 quadrants	0 (0)
Axial length, mm, mean ± SD [range]	25.62 ± 1.96 [22.3 to 29.9]
Refractive errors after surgery, diopters, mean ± SD [range]	
1 mo post	−4.24 ± 4.48 [−18 to 0]
6 mo post	−4.83 ± 4.92 [−17.5 to 0.75]
Preoperative lens status, *n* (%)	
Phakic	19 (95)
Pseudophakic	1 (5)
Preoperative BCVA, logMAR, mean ± SD [range]	1.15 ± 0.51 [0.70 to 2]
Retinal surgery, *n* (%)	
Screral buckling + cryotherapy	7 (35)
with gas tamponade	1 (14)
PPV	13 (75)
Alone	8 (62)
Combined with cataract surgery	5 (38)
With gas tamponade	13 (100)

Statistical Analyses

Statistical analyses were performed by Wilcoxon signed rank tests and Spearman rank correlation tests. The data were analyzed with the Statcel software (Statcel, 3rd edition; OMS, Inc., Tokyo, Japan), which is an add-in module for Microsoft Excel. $P < 0.05$ was considered to be statistically significant.

Results

The demographic and clinical characteristics of the 20 patients (16 men and 4 women) are shown in the Table. The mean ± standard deviation age was 54.5 ± 13.7 years with a range from 26 to 75 years. The mean preoperative BCVA was 1.05 ± 0.62 logMAR units with a range of 0.7 to 2.0 logMAR units. The mean BCVA improved to 0.38 ± 0.21 logMAR units with a range of 0.1 to 0.8 logMAR units at 1 month and 0.28 ± 0.28 logMAR units with a range of 0.0 to 0.8 logMAR units at 6 months postoperatively. The mean refractive errors changed from −4.24 ± 4.48 diopters (D) with a range of −18.00 to 0.00 D at 1 month to −4.83 ± 4.92 D with a range of −17.50 to +0.75 D at 6 months postoperatively.

Seven patients underwent scleral buckling and 13 patients underwent PPV. Cataract surgery was combined with PPV in five eyes.

Representative Cases

Four representative cases of fovea-off RRD with FMERGs and SD-OCT images at 1 and 6 months after surgery are shown in Figure 2. The amplitude of the FMERGs increased postoperatively in all of the cases. The amplitudes of the b-waves of cases 1, 2, and 4 were markedly increased. On the other hand, the amplitude of the b-wave of case 3 increased only slightly.

Spectral-domain OCT showed that the microstructure of the outer photoreceptor layer changed, especially the EZ and CIZ. The ELM was present in almost its full length in most cases already at 1 month. For case 1, the EZ was partially visible at 1 month with a total length of 2650 μm, and it increased to 3869 μm at 6 months. The CIZ was not identified at 1 month and was partially seen at 6 months on the nasal side with a total length of 1260 μm.

In case 2, the EZ was slightly disrupted at 1 month with a total length of 4010 μm, and it was almost fully intact at 6 months with a length of 4470 μm. The CIZ was barely visible throughout the image with a total length 890 μm, and it clearly expanded on the temporal side at 6 months to a total length of 2350 μm.

In case 3, the EZ was faint and disrupted with a total length of 3550 μm at 1 month and almost fully intact at 6 months with a length of 4450 μm. The CIZ was barely visible in the temporal retina with a total length of 750 μm, and it became clearer at 6 months with a total length of 1070 μm.

In case 4, subretinal fluid was still present at 1 and 6 months. The b-wave amplitude of case 4 almost doubled at 6 months in spite of the presence of subretinal fluid. The EZ was visible throughout the image at both time points, but it was indistinct and thickened especially in the area of the retinal detachment. The CIZ was partially visible at 6 months, but it was difficult to evaluate its appearance in the area with subretinal fluid. Thus, we excluded the four cases with subretinal fluid and two cases with cystoid macular edema from the SD-OCT analyses.

Focal Macular Electroretinograms

The components of the FMERGs of the affected and fellow eyes of the 20 patients at 1 and 6 months after the surgery are shown in Figure 3. The implicit times of the a-waves were not significantly different between 1 and 6 months after the surgery. The implicit times of the b-waves were significantly shorter by 1.5 ms at 6 months than at 1 month after the surgery ($P < 0.01$). The implicit times of the a- and b-waves at 1 and 6 months after surgery were significantly longer than those of the fellow eyes (Figs. 3A, 3B). The amplitudes of the a- and b-waves at 6 months after surgery increased significantly by 1.4 and 1.7 times that at 1 month after the surgery ($P < 0.01$, $P < 0.001$, respectively). However, these values did not recover to the level of the fellow eyes (Figs. 3C, 3D).

SD-OCT Measurements

The results of SD-OCT at 1 and 6 months postoperatively are shown in Figure 4. The quality of all of the OCT images was high enough to analyze the morphology of the outer retinal layer. For these analyses, we excluded six cases that had residual subretinal fluid or cystoid macular edema at 1 month because it prevented an accurate measurement of the images. In the end, the SD-OCT images from 14 patients were analyzed.

On the average, 97.4% (4384 μm/4500 μm) of the ELM length was detected at 1 month after the surgery, and it did not significantly change at 6 months. The lengths of the ELM of the affected eyes at 1 and 6 months were not significantly different from those of the fellow eyes.

The mean length of the EZ was 3554.71 ± 598.23 μm (mean ± SD) at 1 month, which was approximately 79% of the analyzed length, and it increased significantly to 4191.41 ± 276.2 μm at 6 months ($P < 0.001$). However, the mean length

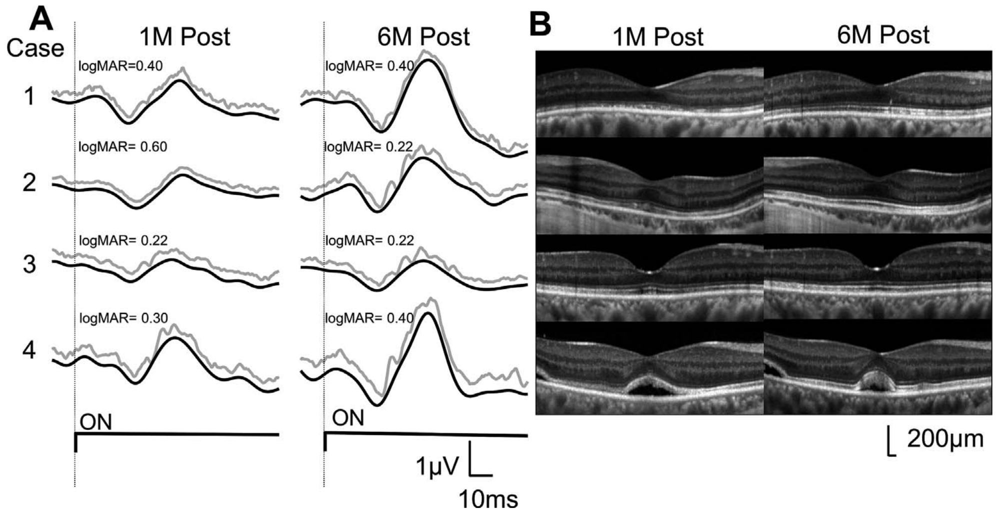

FIGURE 2. Focal macular ERGs (FMERGs) elicited from 15° of the macular area (**A**) and SD-OCT images (**B**) at 1 and 6 months after surgery of four representative cases. The images recorded 1 month after the surgery are shown on the *left*, and those recorded 6 months after the surgery are shown on the *right*. (**A**) FMERGs after filtering frequencies > 70 Hz by Fast Fourier Transform (FFT) are shown beneath the original wave. The FMERGs are increased after surgery to different degrees. Case 3 had a slight increase, but the other cases increased markedly. (**B**) The SD-OCT images show microstructural changes in the outer photoreceptor layers in all cases. Case 1 has a marked elongation of the EZ and CIZ. Case 2 has a slight elongation of the EZ and marked elongation of the CIZ. Case 3 has a moderate elongation of the EZ and slight elongation of CIZ, and case 4 has retained subretinal fluid.

at 6 months was still less than that of the fellow eyes at 4476.86 ± 63.38 μm.

The mean length of the CIZ was 746.29 ± 847.76 μm at 1 month, which was 16.5% of the analyzed length, and it increased significantly to 1436.35 ± 901.10 μm at 6 months ($P < 0.001$). The mean length of the CIZ in the fellow eyes was 4107.36 ± 677.23, which indicated that 9% of the CIZ was not detected even in the healthy fellow eyes.

The mean outer photoreceptor area at 1 month was 1.04 ± 0.07 mm^2, and it increased significantly to 1.36 ± 0.10 mm^2 at 6 months ($P < 0.01$). At this time, it was not significantly different from that of the fellow eyes (1.47 ± 0.15 mm^2).

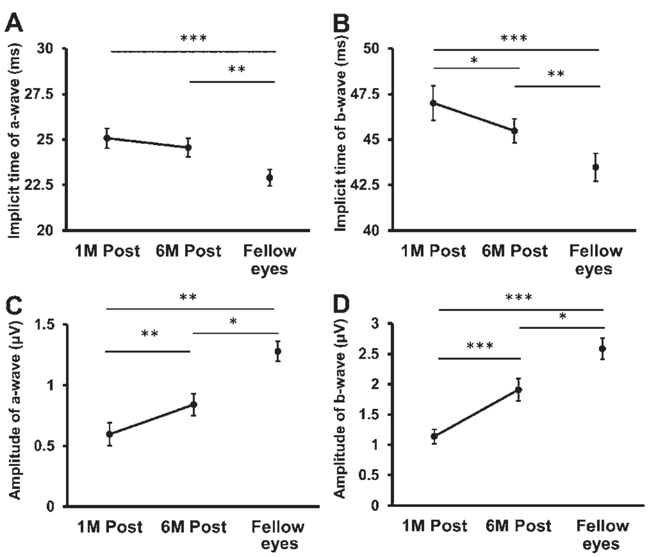

FIGURE 3. Components of the focal macular ERGs (FMERGs) of 20 affected eyes at 1 and 6 months after the surgery and those of the fellow eyes. (**A**) Implicit times of the a-waves. (**B**) Implicit times of the b-waves. (**C**) Amplitudes of the a-waves. (**D**) Amplitudes of the b-waves. The implicit times of the b-waves and the amplitudes of the a- and b-waves at postoperative 6 months changed significantly compared to those at postoperative 1 month (**B**–**D**) (*$P < 0.05$, **$P < 0.01$, ***$P < 0.001$; Wilcoxon signed rank tests).

Correlation Between Changes of Outer Retinal Morphology and Improvements of FMERG Components After Successful Surgery for Fovea-Off RRD

Next, we determined whether the improvement of the FMERGs was significantly correlated with the changes of the microstructures of the photoreceptor layer at 1 and 6 months postoperatively in 14 eyes. The differences in the values of the

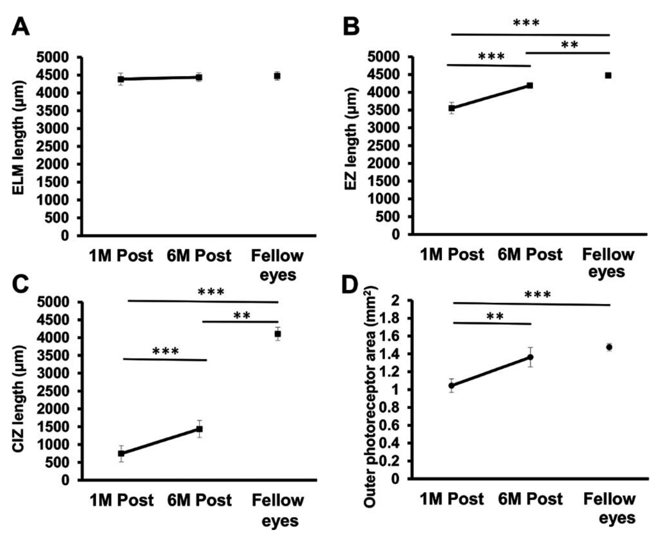

FIGURE 4. Outer photoreceptor microstructures in the SD-OCT images at 1 and 6 months after surgery and those of the fellow eyes. (**A**) ELM length, (**B**) EZ length, (**C**) CIZ length, (**D**) outer photoreceptor area. The EZ length, CIZ length, and outer photoreceptor area at postoperative 1 month are significantly larger than those at postoperative 6 months (**$P < 0.01$, ***$P < 0.001$; Wilcoxon signed rank tests).

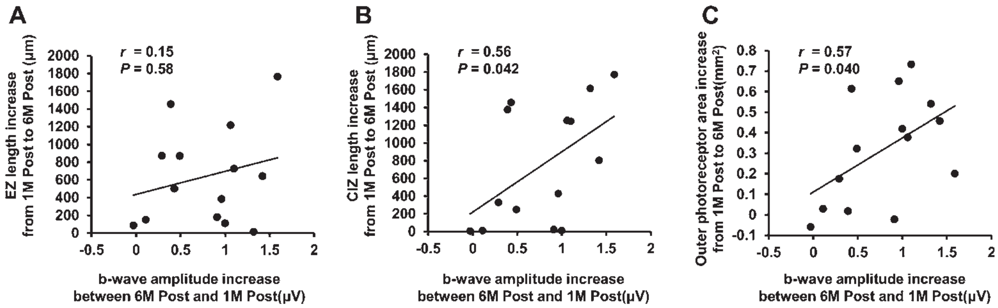

Figure 5. Correlations between the SD-OCT parameters (6M Post − 1M Post) and the amplitudes of the FMERG b-waves (6M Post − 1M Post). The changes of amplitudes of the b-waves were significantly correlated with the CIZ length (**B**) and the outer photoreceptor area (**C**), but the increase in amplitude of the b-wave was not significantly correlated with the increase in EZ length (**A**) (Spearman rank correlation test).

SD-OCT components between 1 and 6 months after surgery were not significantly correlated with the changes of the amplitudes of the a-waves (Supplementary Fig. S1) and the implicit times of the b-waves (Supplementary Fig. S2) of the FMERGs. The increase in the length of the CIZ and outer photoreceptor area was significantly correlated with the amplitudes of the b-waves ($r = 0.56$, $P = 0.042$ for the CIZ; $r = 0.57$, $P = 0.040$ for the outer photoreceptor area). However, the increase in the length of the EZ was not significantly correlated with the amplitudes of the b-waves ($r = 0.15$, $P = 0.58$; Fig. 5).

We also determined whether the values of OCT parameters were correlated with the amplitude of FMERG b-wave at postoperative 1 and 6 months in 14 eyes. Our results showed that the amplitudes of the b-waves were not significantly correlated with the length of the EZ, CIZ, and the outer photoreceptor area at both time points (Supplementary Fig. S3).

Discussion

Our results showed that there were restorations of the microstructures of the photoreceptor layer, including the EZ, CIZ, and outer photoreceptor area, after successful surgery for fovea-off RRD. The restoration of the CIZ and increase in the outer photoreceptor area were significantly correlated with the increase in the amplitudes of the b-waves of the FMERGs during the 5-month follow-up period.

Our results are in good agreement with earlier findings that the length of the EZ and CIZ and the size of the outer photoreceptor layer increase during the follow-up period. Also, a significant correlation between the BCVA and the increase in the ELM–RPE distance has been reported in earlier studies.[19,21] This might be similar to our results on the correlations between the increase of the outer photoreceptor area and the increase of FMERG b-wave amplitude.

An interesting finding was that the increase in the amplitudes of the FMERG b-waves was significantly correlated with the increase in the length of the CIZ, and little change in the FMERG was consistent with lack of change in CIZ. However, the increase in the amplitudes of FMERGs was not significantly correlated with the increase in the EZ length. This indicates that the increases of the FMERG b-waves were accompanied by the CIZ recovery as shown in cases 1 and 2. On the other hand, the postoperative length of the EZ was not correlated with the amplitudes of the FMERGs, with little increase of the length of the CIZ as shown in case 3. The CIZ is part of the photoreceptor outer segments, and the EZ is part of the inner segments. Usually the CIZ is visible only after the EZ is restored because the photoreceptor outer segments regenerate after the inner segments are formed. Thus, we postulate that a restoration of the EZ alone is not enough to improve the FMERGs and a restoration of the EZ accompanied by that of the CIZ is necessary for improvements of the FMERGs.

Many earlier OCT studies reported that the integrity of EZ was correlated with visual acuities and retinal sensitivities after successful retinal reattachment.[3,5,13–16] Our results appear to be inconsistent with these earlier reports; however, those papers did not assess the status of the CIZ, and we assume that the patients whose EZ was accompanied with improvement of the CIZ had good BCVA. Supporting our assumption, Gharbiya et al.[18] reported that the status of CIZ was an important predictor of postoperative BCVA, and the CIZ appeared to be even more sensitive than the EZ in predicting the BCVA after successful RRD repair.

The visual acuity of some patients did not recover during the follow-up period even though the amplitudes of b-waves significantly recovered, as in cases 1 and 4 in Figure 2. Significant correlations between the visual acuity improvement and change of FMERG components were not found in this study (data not shown). Furthermore, there were no significant correlations between visual acuity improvements and the changes of the EZ, CIZ, and outer photoreceptor area during follow-up periods (data not shown).

Several studies have reported that a foveal bulge, which is an upward deflection of the ELM, EZ, and CIZ in the central fovea, was a good marker of good BCVA after successful recovery of the RRD.[19,21] A good BCVA depends on the function of the central fovea, and it might be more appropriate to evaluate the foveal bulge than the integrity of the entire EZ in assessing the BCVA. A foveal bulge was detected in seven patients and was not detected in seven patients in the SD-OCT images at 6 months after surgery. We compared the amplitudes of the FMERG b-waves between the two groups, but there was no significant difference (data not shown). These findings indicated that the FMERGs do not represent the function of the central fovea.

A significant correlation was reported between the length of the CIZ and the amplitudes of the FMERGs in other diseases. Occult macular dystrophy (OMD) is a hereditary retinal disease with normal fundus appearances in spite of a slow progressive decrease of the visual acuity.[36] The diagnosis of OMD is based on reduced amplitudes of the FMERGs and/or multifocal ERGs. Even though the fundus of OMD patients appears normal, recent studies reported the presence of EZ but the absence of CIZ in the SD-OCT images in most of the cases.[37–40] This condition might indicate that the CIZ is essential for generating the electrical potentials from the photoreceptors in the macular area.

Our results showed that the amplitudes of the b-waves at both 1 and 6 months were not significantly correlated with the length of the EZ and CIZ and outer photoreceptor area as shown in Supplementary Figure S3. These results appear to be inconsistent with the data indicating that the increases in the CIZ and outer photoreceptor area were significantly correlated with the increase in the amplitude of FMERG b-wave after surgery. Because the FMERG amplitudes are also influenced by other factors, such as the axial length and bipolar cell function, we suggest that the evaluation of the differences of the FMERGs between 1 and 6 months probably cancelled these factors. Therefore, evaluation of the difference between 1 and 6 months might be a more sensitive way to detect the correlations between OCT parameters and FMERG amplitudes. We also suggest that a larger sample size is needed to analyze the correlation between the OCT parameters and the FMERG b-wave amplitudes.

Increases in both the a- and b-wave amplitudes during the follow-up period indicated that the number of cones that evoke the electric potentials increased. But the delay of the implicit times of both the a- and b-waves even at 6 months postoperatively suggests that the function of the cones had not fully recovered. Electrical activities of FMERG b-waves are known to reflect mainly activity of retinal ON-bipolar cells, which are transmitted signals from photoreceptors.[41] Our results on the significant correlation of the restoration of the CIZ with increase in the amplitudes of the b-waves of the FMERGs indicate that the improvements of the amplitudes of b-waves reflected the restoration of photoreceptors rather than improvement of retinal ON-bipolar cell function.

On the other hand, the changes in the amplitudes of a-waves of FMERG were not significantly correlated with the changes in SD-OCT components (Supplementary Fig. S1). The reasons for this were not determined, but the amplitudes of a-waves might be too small and variable to show significant correlations with SD-OCT changes.

There are several limitations in this study. This was a retrospective study and the sample size was relatively small. In addition, the inclusion of both PPV and scleral buckling might have affected the results. Several studies have reported that the recovery course in eyes treated with PPV and scleral buckling was different.[22,42] However, we believe that the restoration of the CIZ is necessary for improving the amplitudes of the FMERGs by either procedure.

We also excluded cases with subretinal fluid due to a difficulty in measuring the length of the CIZ. However, as shown in Figure 2, some cases with subretinal fluid had an increase in the amplitude of the FMERGs. Several groups have reported that 15% to 50% of cases after RRD repair had subretinal fluid, and the postoperative BCVA was not associated with the duration and extent of the subretinal fluid.[5,13,16,43,44] Additional studies to determine the relationship of the function and microstructures of patients with subretinal fluid are needed.

It has been reported that the ELM, EZ, and CIZ may appear fragmented or even absent in healthy eyes as a result of recording artifacts.[45] In fact, the CIZ was missing in 9% of the fellow eyes in our patients, which might indicate that measuring the length of the CIZ in operated eyes needs to be considered as yielding false negatives.

In conclusion, we showed that the amplitudes and implicit times of the FMERGs improved significantly after reattachment of the retina in eyes with fovea-off RRD. The improvements of FMERG b-waves were significantly correlated with the increase of the length of the CIZ but not with that of the EZ. Restoration of the EZ alone might not be enough to improve the FMERGs, and a restoration of the length of the EZ accompanied by that of the CIZ was essential for the recovery of the FMERGs after repair of fovea-off RRD.

Acknowledgments

Supported by the Scientific Research C fund (25462709 SU) from Ministry of Education, Culture, Sports, Science and Technology of Japan.

Disclosure: **A. Kominami**, None; **S. Ueno**, None; **T. Kominami**, None; **A. Nakanishi**, None; **C.-H. Piao**, None; **E. Ra**, None; **S. Yasuda**, None; **T. Asami**, None; **H. Terasaki**, None

References

1. Sharma YR, Karunanithi S, Azad RV, et al. Functional and anatomic outcome of scleral buckling versus primary vitrectomy in pseudophakic retinal detachment. *Acta Ophthalmol Scand*. 2005;83:293–297.
2. Adelman RA, Parnes AJ, Ducournau D; European Vitreo-Retinal Society (EVRS) Retinal Detachment Study Group. Strategy for the management of uncomplicated retinal detachments: the European vitreo-retinal society retinal detachment study report 1. *Ophthalmology*. 2013;120:1804–1808.
3. Delolme MP, Dugas B, Nicot F, Muselier A, Bron AM, Creuzot-Garcher C. Anatomical and functional macular changes after rhegmatogenous retinal detachment with macula off. *Am J Ophthalmol*. 2012;153:128–136.
4. Salicone A, Smiddy WE, Venkatraman A, Feuer W. Visual recovery after scleral buckling procedure for retinal detachment. *Ophthalmology*. 2006;113:1734–1742.
5. Shimoda Y, Sano M, Hashimoto H, Yokota Y, Kishi S. Restoration of photoreceptor outer segment after vitrectomy for retinal detachment. *Am J Ophthalmol*. 2010;149:284–290.
6. Kang HM, Lee SC, Lee CS. Association of spectral-domain optical coherence tomography findings with visual outcome of macula-off rhegmatogenous retinal detachment surgery. *Ophthalmologica*. 2015;234:83–90.
7. Dell'Omo R, Mura M. Metamorphopsia and optical coherence tomography findings after rhegmatogenous retinal detachment surgery. *Am J Ophthalmol*. 2014;157:1322–1323.
8. Kroll AJ, Machemer R. Experimental retinal detachment in the owl monkey. 3. Electron microscopy of retina and pigment epithelium. *Am J Ophthalmol*. 1968;66:410–427.
9. Lewis GP, Charteris DG, Sethi CS, Fisher SK. Animal models of retinal detachment and reattachment: identifying cellular events that may affect visual recovery. *Eye*. 2002;16:375–387.
10. Cook B, Lewis GP, Fisher SK, Adler R. Apoptotic photoreceptor degeneration in experimental retinal detachment. *Invest Ophthalmol Vis Sci*. 1995;36:990–996.
11. Hisatomi T, Sakamoto T, Goto Y, et al. Critical role of photoreceptor apoptosis in functional damage after retinal detachment. *Curr Eye Res*. 2002;24:161–172.
12. Arroyo JG, Yang L, Bula D, Chen DF. Photoreceptor apoptosis in human retinal detachment. *Am J Ophthalmol*. 2005;139:605–610.
13. Schocket LS, Witkin AJ, Fujimoto JG, et al. Ultrahigh-resolution optical coherence tomography in patients with decreased visual acuity after retinal detachment repair. *Ophthalmology*. 2006;113:666–672.
14. Smith AJ, Telander DG, Zawadzki RJ, et al. High-resolution Fourier-domain optical coherence tomography and microperimetric findings after macula-off retinal detachment repair. *Ophthalmology*. 2008;115:1923–1929.
15. Nakanishi H, Hangai M, Unoki N, et al. Spectral-domain optical coherence tomography imaging of the detached macula in rhegmatogenous retinal detachment. *Retina*. 2009;29:232–242.

16. Wakabayashi T, Oshima Y, Fujimoto H, et al. Foveal microstructure and visual acuity after retinal detachment repair: imaging analysis by Fourier-domain optical coherence tomography. *Ophthalmology*. 2009;116:519–528.
17. Lai WW, Leung GY, Chan CW, Yeung IY, Wong D. Simultaneous spectral domain OCT and fundus autofluorescence imaging of the macula and microperimetric correspondence after successful repair of rhegmatogenous retinal detachment. *Br J Ophthalmol*. 2010;94:311–318.
18. Gharbiya M, Grandinetti F, Scavella V, et al. Correlation between spectral-domain optical coherence tomography findings and visual outcome after primary rhegmatogenous retinal detachment repair. *Retina*. 2012;32:43–53.
19. Hasegawa T, Ueda T, Okamoto M, Ogata N. Relationship between presence of foveal bulge in optical coherence tomographic images and visual acuity after rhegmatogenous retinal detachment repair. *Retina*. 2014;34:1848–1853.
20. Menke MN, Kowal JH, Dufour P, et al. Retinal layer measurements after successful macula-off retinal detachment repair using optical coherence tomography. *Invest Ophthalmol Vis Sci*. 2014;55:6575–6579.
21. dell'Omo R, Viggiano D, Giorgio D, et al. Restoration of foveal thickness and architecture after macula-off retinal detachment repair. *Invest Ophthalmol Vis Sci*. 2015;56:1040–1050.
22. Baba T, Mizuno S, Tatsumi T, et al. Outer retinal thickness and retinal sensitivity in macula-off rhegmatogenous retinal detachment after successful reattachment. *Eur J Ophthalmol*. 2012;22:1032–1038.
23. Azarmina M, Moradian S, Azarmina H. Electroretinographic changes following retinal reattachment surgery. *J Ophthalmic Vis Res*. 2013;8:321–329.
24. Sasoh M, Yoshida S, Kuze M, Uji Y. The multifocal electroretinogram in retinal detachment. *Doc Ophthalmol*. 1997;94:239–252.
25. Moschos M, Mallias J, Ladas I, et al. Multifocal ERG in retinal detachment surgery. *Eur J Ophthalmol*. 2001;11:296–300.
26. Wu D, Gao R, Zhang G, Wu L. Comparison of pre- and post-operational multifocal electroretinograms of retinal detachment. *Chin Med J. (Engl)*. 2002;115:1560–1563.
27. Schatz P, Holm K, Andreasson S. Retinal function after scleral buckling for recent onset rhegmatogenous retinal detachment: assessment with electroretinography and optical coherence tomography. *Retina*. 2007;27:30–36.
28. Miyake Y. Studies of local macular ERG [in Japanese]. *Nihon Ganka Gakkai Zasshi*. 1988;92:1419–1449.
29. Terasaki H, Kojima T, Niwa H, et al. Changes in focal macular electroretinograms and foveal thickness after vitrectomy for diabetic macular edema. *Invest Ophthalmol Vis Sci*. 2003;44:4465–4472.
30. Ishikawa K, Kondo M, Ito Y, et al. Correlation between focal macular electroretinograms and angiographic findings after photodynamic therapy. *Invest Ophthalmol Vis Sci*. 2007;48:2254–2259.
31. Iwata E, Ueno S, Ishikawa K, et al. Focal macular electroretinograms after intravitreal injections of bevacizumab for age-related macular degeneration. *Invest Ophthalmol Vis Sci*. 2012;53:4185–4190.
32. Hibi N, Ueno S, Ito Y, et al. Relationship between retinal layer thickness and focal macular electroretinogram components after epiretinal membrane surgery. *Invest Ophthalmol Vis Sci*. 2013;54:7207–7214.
33. Ueno S, Koyasu T, Kominami T, et al. Focal cone ERGs of rhodopsin Pro347Leu transgenic rabbits. *Vision Res*. 2013;91:118–123.
34. Ueno S, Nakanishi A, Nishi K, Suzuki S, Terasaki H. Case of paraneoplastic retinopathy with retinal ON-bipolar cell dysfunction and subsequent resolution of ERGs. *Doc Ophthalmol*. 2015;130:71–76.
35. Schneider CA, Rasband WS, Eliceiri KW. NIH Image to ImageJ: 25 years of image analysis. *Nat Methods*. 2012;9:671–675.
36. Miyake Y, Ichikawa K, Shiose Y, Kawase Y. Hereditary macular dystrophy without visible fundus abnormality. *Am J Ophthalmol*. 1989;108:292–299.
37. Tsunoda K, Usui T, Hatase T, et al. Clinical characteristics of occult macular dystrophy in family with mutation of RP1l1 gene. *Retina*. 2012;32:1135–1147.
38. Ahn SJ, Cho SI, Ahn J, et al. Clinical and genetic characteristics of Korean occult macular dystrophy patients. *Invest Ophthalmol Vis Sci*. 2013;54:4856–4863.
39. Nakanishi A, Ueno S, Kawano K, et al. Pathologic changes of cone photoreceptors in eyes with occult macular dystrophy. *Invest Ophthalmol Vis Sci*. 2015;56:7243–7249.
40. Chen CJ, Scholl HP, Birch DG, et al. Characterizing the phenotype and genotype of a family with occult macular dystrophy. *Arch Ophthalmol*. 2012;130:1544–1549.
41. Kondo M, Ueno S, Piao CH, Miyake Y, Terasaki H. Comparison of focal macular cone ERGs in complete-type congenital stationary night blindness and APB-treated monkeys. *Vision Res*. 2008;48:273–280.
42. Schatz P, Andreasson S. Recovery of retinal function after recent-onset rhegmatogenous retinal detachment in relation to type of surgery. *Retina*. 2010;30:152–159.
43. Hagimura N, Iida T, Suto K, Kishi S. Persistent foveal retinal detachment after successful rhegmatogenous retinal detachment surgery. *Am J Ophthalmol*. 2002;133:516–520.
44. Seo JH, Woo SJ, Park KH, Yu YS, Chung H. Influence of persistent submacular fluid on visual outcome after successful scleral buckle surgery for macula-off retinal detachment. *Am J Ophthalmol*. 2008;145:915–922.
45. Rii T, Itoh Y, Inoue M, Hirakata A. Foveal cone outer segment tips line and disruption artifacts in spectral-domain optical coherence tomographic images of normal eyes. *Am J Ophthalmol*. 2012;153:524–529.